



Published in final edited form as:

*Neurobiol Aging*. 2013 August ; 34(8): 2052–2063. doi:10.1016/j.neurobiolaging.2013.02.015.

## A small molecule p75<sup>NTR</sup> ligand prevents cognitive deficits and neurite degeneration in an Alzheimer's mouse model

Juliet K. Knowles<sup>a,b</sup>, Danielle A. Simmons<sup>a,#</sup>, Thuy-Vi V. Nguyen<sup>a,#</sup>, Lilith Vander Griend<sup>a</sup>, Youmei Xie<sup>b</sup>, Hong Zhang<sup>c</sup>, Tao Yang<sup>a</sup>, Julia Pollak<sup>a</sup>, Timothy Chang<sup>a</sup>, Ottavio Arancio<sup>c</sup>, Marion S. Buckwalter<sup>a</sup>, Tony Wyss-Coray<sup>a,d</sup>, Stephen M. Massa<sup>e,f,g</sup>, Frank M. Longo<sup>a,\*</sup>

<sup>a</sup>Department of Neurology and Neurological Science, Stanford University, Stanford, CA, USA

<sup>b</sup>Department of Neurology, University of North Carolina-Chapel Hill, Chapel Hill, NC, USA

<sup>c</sup>Department of Pathology and Taub Institute, Columbia University, New York, NY, USA

<sup>d</sup>Palo Alto Veterans Affairs Health Care System, Palo Alto, CA, USA

<sup>e</sup>Department of Neurology, San Francisco Veterans Affairs Medical Center, San Francisco, CA, USA

<sup>f</sup>Laboratory for Computational Neurochemistry and Drug Discovery, San Francisco Veterans Affairs Medical Center, San Francisco, CA, USA

<sup>g</sup>Department of Neurology, University of California–San Francisco, San Francisco, CA, USA

### Abstract

The p75 neurotrophin receptor (p75<sup>NTR</sup>) is associated with multiple mechanisms linked to Alzheimer's disease (AD); hence, modulating its function might confer therapeutic effects. In previous *in vitro* work, we developed small molecule p75<sup>NTR</sup> ligands that inhibited amyloid- $\beta$ -induced degenerative signaling and prevented neurite degeneration. In the present study, a prototype p75<sup>NTR</sup> ligand, LM11A-31, was administered orally to the Thy-1 hAPP<sup>Lond/Swe</sup> (APP<sup>L/S</sup>) AD mouse model. LM11A-31 reached brain concentrations known to inhibit degenerative signaling without toxicity or induction of hyperalgesia. It prevented deficits in novel object recognition after 2.5 months and, in a separate cohort, deficits in Y-maze performance after 3 months of treatment. Stereology studies found that the number and size of basal forebrain cholinergic neurons, which are normal in APP<sup>L/S</sup> mice, were unaffected. Neuritic dystrophy, however, was readily apparent in the basal forebrain, hippocampus and cortex, and was significantly reduced by LM11A-31, with no effect on amyloid levels. These studies reveal

Open access under [CC BY-NC-ND license](#).

\*Corresponding author at: Department of Neurology and Neurological Sciences, Stanford University, Palo Alto, CA 94304. Tel.: +650 724-3172; fax: +650 498-4579. [longo@stanford.edu](mailto:longo@stanford.edu) (F.M. Longo).

#D.A.S. and T.-V.V.N. are co-second authors and contributed equally to this work.

Disclosure statement

F.M.L. is a founder of and retains financial interest in Pharmatrophix, a company focused on the development of small molecule ligands for neurotrophin receptors. Otherwise there are no conflicts of interest.

Appendix A. Supplementary data

Supplementary data associated with this article can be found, in the online version, at <http://dx.doi.org/10.1016/j.neurobiolaging.2013.02.015>

that p75<sup>NTR</sup> is an important and tractable in vivo drug target for AD, with LM11A-31 representing a novel class of therapeutic candidates.

## Keywords

Alzheimers' disease; p75 neurotrophin receptor; Neuritic dystrophy; LM11A-31

---

## 1. Introduction

Although reduction of amyloid- $\beta$  (A $\beta$ ) levels during early disease stages remains an important goal in the treatment of Alzheimer's disease (AD), effective therapies will likely require parallel approaches for mitigating neurodegeneration (Longo and Massa, 2004). Therapeutic strategies capable of simultaneously affecting multiple AD-induced neurodegenerative mechanisms are more likely to be efficacious. This goal could be achieved by upstream targeting of receptors at the apices of pertinent signaling cascades; however, few receptors have been identified that are directly linked to multiple nodes of signaling networks contributing to AD.

Multiple lines of evidence suggest that one such target is the p75 neurotrophin receptor (p75<sup>NTR</sup>). P75<sup>NTR</sup> binds pro-nerve growth factor (proNGF) and NGF together with co-receptors including Trk and sortilin (Lee et al., 2001; Teng et al., 2010). It may promote either degenerative or survival signaling depending on the type and level of its ligand, the presence or absence of co-receptors, and other factors (Barker, 2004; Dechant and Barde, 2002; Ibanez and Simi, 2012; Underwood and Coulson, 2008). Expression of p75<sup>NTR</sup> in cell lines allows or enhances A $\beta$ -induced toxicity, suggestive of an enabling role in AD (Perini et al., 2002; Rabizadeh et al., 1994; Yaar et al., 1997). P75<sup>NTR</sup> is expressed by neurons known to degenerate in AD, including basal forebrain cholinergic, entorhinal, hippocampal, cortical, and locus coeruleus neurons, and its expression is increased in the AD brain (Bruns and Miller, 2007; Chakravarthy et al., 2010; Chakravarthy et al., 2012; Dougherty and Milner, 1999; Jacobs and Miller, 1999; Longo and Massa, 2005; Mufson and Kordower, 1992). The role of NGF signaling through p75<sup>NTR</sup> and TrkA in regulating the trophic status of basal forebrain cholinergic neurons (BFCNs) has been particularly well characterized in developing (Greferath et al., 2000; Naumann et al., 2002; Yeo et al., 1997), aging (Longo and Massa, 2004; Sofroniew et al., 2001), and AD brains (Mufson et al., 2008; Schliebs and Arendt, 2011). BFCN loss occurred when A $\beta$  oligomers were infused into the brains of wild-type, but not p75<sup>NTR</sup>  $-/-$ , mice (Sotthibundhu et al., 2008), and removal of exon III of p75<sup>NTR</sup> (which deletes its neurotrophin binding domain) in the Thy-1 hAPP<sup>Lond/Swe</sup> (APP<sup>L/S</sup>) mouse model of AD prevented BFCN neurite degeneration (Knowles et al., 2009). Given these findings in murine models, it is notable that in mild cognitive impairment (MCI) and AD, degeneration of BFCN neurites precedes neuron loss and correlates with loss of cognitive function (Vana et al., 2011). An increased ratio of p75<sup>NTR</sup> to TrkA expression is thought to contribute to degenerative signaling in AD-affected BFCNs (Diarra et al., 2009; Ginsberg et al., 2006). The underlying mechanisms likely involve p75<sup>NTR</sup> modulation of tau phosphorylation (through cdk5 and GSK3 $\beta$ ), synaptic function and spine stability (through

PKC/CREB and RhoA), and neuronal degeneration (through JNK and AKT) (Coulson, 2006; James et al., 2008; Longo and Massa, 2005; Yang et al., 2008).

Past attempts to apply NGF as an AD therapeutic were limited by its poor stability and bioavailability, requiring intrathecal administration, and serious side effects occurred in human subjects, including weight loss and pain (Eriksdotter Jonhagen et al., 1998). NGF-induced weight loss and hyperalgesia has been characterized in murine and other animal models, and signaling through TrkA expressed on dorsal root ganglion cells is one of several potential mechanisms contributing to hyperalgesia (Bergmann et al., 1998; Ugolini et al., 2007). Although NGF can promote survival or enhance trophic status in BFCN neurons (Hefti and Weiner, 1986; Kromer, 1987; Sofroniew et al., 2001; Tuszynski et al., 1990; Williams et al., 1986), it may be toxic to other neuron populations, particularly those expressing high p75<sup>NTR</sup> to TrkA ratios (Friedman, 2000; Roux and Barker, 2002), which are more likely to be present in the AD brain (Mufson et al., 1996; Mufson et al., 1997; Mufson et al., 2008).

With regard to these challenges, we identified a collection of non-peptide small molecules with selected structural and physical chemical features of the NGF loop 1 domain (known to interact with p75<sup>NTR</sup>) by in silico and in vitro screening of small molecule libraries (Massa et al., 2006). These small molecules were found to compete with NGF and proNGF binding to p75<sup>NTR</sup> but not to TrkA (Massa et al., 2006). They activated AKT and prevented death of cultured hippocampal neurons; both effects were entirely dependent upon the expression of p75<sup>NTR</sup>, and trophic effects were blocked by antibodies directed against the p75<sup>NTR</sup> extracellular domain. LM11A-31, a lead small molecule emerging from that work, is a water-soluble isoleucine derivative containing a morpholino group (MW 243.3), the structure of which was originally published by Massa et al. (2006) (Supplementary Fig. 1). In in vitro studies, we found that LM11A-31 inhibited A $\beta$ -induced degeneration in a p75<sup>NTR</sup>-dependent manner. LM11A-31 blocked A $\beta$ -induced activation of GSK3 $\beta$ , cdk5, and JNK; it inhibited the ability of A $\beta$  to block activation of AKT and CREB; and it prevented excess tau phosphorylation (Yang et al., 2008). Interestingly, in these studies, NGF failed to prevent A $\beta$ -induced neuronal death and activation of GSK3 $\beta$  and c-Jun. This indicates that LM11A-31 modulates p75<sup>NTR</sup> signaling in a mode distinct from that of NGF, and that it represents a novel approach to targeting p75<sup>NTR</sup> in AD. In addition, small molecule, non-peptide compounds such as LM11A-31 have the potential for enhanced stability and brain bioavailability, making them amenable to systemic administration at lower doses.

In the present study, we determined whether oral administration of LM11A-31 would lead to therapeutic brain levels without promoting the deleterious NGF-related effects of weight loss or lowered pain threshold. Furthermore, we determined whether LM11A-31 could prevent cognitive impairment and neurodegeneration in the APP<sup>L/S</sup> mouse model of AD. In this line, amyloid plaques are first present in the frontal cortex at 3 to 4 months of age, and mature plaques containing dystrophic neurites are present in the frontal cortex, hippocampus, thalamus, and olfactory region by 5 to 7 months of age (Rockenstein et al., 2001). Synapse loss parallels the spread of plaques, becoming apparent in the frontal cortex and hippocampus by 5 to 7 months of age and progressing thereafter (Rockenstein et al., 2001). During the 6- to 9-month age period, p75<sup>NTR</sup> levels in the hippocampus and basal

forebrain of APP<sup>L/S</sup> mice are unaltered (T.-V.V. Nguyen and D.A. Simmons, unpublished data). Based on the established timeline of pathologic changes in APP<sup>L/S</sup> mice (Rockenstein et al., 2001), our previous studies showing that crossing APP<sup>L/S</sup> mice with p75<sup>NTR</sup> exon III <sup>-/-</sup> mice leads to decreased neuritic degeneration at 5 to 7 months of age (Knowles et al., 2009), and the likelihood that degeneration of neurites is an important contributor to cognitive deficits in AD (Knowles et al., 1999; Vana et al., 2011), we designed a trial to determine whether treatment of APP<sup>L/S</sup> mice in early stages of pathology can reduce disease progression. Reduction of neurite degeneration and behavioral deficits were defined as two pre-hoc primary endpoints to assess LM11A-31 therapeutic potential and hence validation of p75<sup>NTR</sup> as a therapeutic target.

## 2. Methods

### 2.1. Pharmacokinetic/toxicology studies of LM11A-31

Pharmacokinetic and toxicology studies were conducted at Absorption Systems (Exton PA) with the approval of the Institutional Animal Care and Use Committee or at the Palo Alto Veteran's Administration Hospital with approval of the Committee on Animal Research. CNS bioavailability of LM11A-31 was assessed in male CD-1 mice (a standardized model for blood-brain barrier penetration) and female C57BL/6 mice (background strain for the APP<sup>L/S</sup> mice used here). LM11A-31 [2-amino-3-methyl-pentanoic acid (2-morpholin-4-yl-ethyl)-amide, structure provided in Supplementary Fig. 1], was custom synthesized by AMRI (Albany, NY) or Ricerca Biosciences (Painesville, OH) at greater than 97% purity as assessed by liquid chromatography/mass spectroscopy (LC-MS) analysis. In addition, all lots of LM11A-31 were tested for bioactivity (increased hippocampal neuron survival) in cell culture as characterized in previous work (Massa et al., 2006). Before dosing, LM11A-31 was dissolved in sterile filtered water and was administered over a range of doses by oral gavage or intraperitoneal injection. Before sacrifice, mice were anesthetized with a lethal dose of 2.8% chloral hydrate, and 300 to 800  $\mu$ L blood was collected by cardiac puncture with a heparin or ethylenediaminetetraacetic acid (EDTA)-coated needle. Blood samples were centrifuged at  $1000 \times g$  for 15 minutes, and plasma was collected and stored at  $-80^{\circ}\text{C}$  before analysis. In some cases, atenolol (Sigma, St. Louis, MO), a drug with poor CNS penetration, served as a control for blood contamination of brain tissue and was administered  $\sim$ 1 hour before sacrifice by oral gavage. After blood was obtained, the whole brain was dissected and placed immediately on dry ice and stored at  $-80^{\circ}\text{C}$  until LC-MS analysis for LM11A-31 and atenolol. Test accuracy was verified by generating a standard curve, in which known amounts of LM11A-31 were added to blank brain extract.

### 2.2. Open field test

All behavioral analyses were conducted at the Palo Alto Veteran's Administration Hospital with approval of the Committee on Animal Research. A summary of the mice used in this and all other studies in this manuscript is provided in Supplementary Table 1. Female C57BL/6 mice underwent open field testing after 9 days of dosing with 0, 10 or 50 mg/kg/day of LM11A-31. These studies used a  $16 \times 16 \times 15$ -inch photobeam activity box system (San Diego Instruments, San Diego, CA). Ambulatory events were defined as single beam breaks; fine movements, including behaviors such as grooming, were defined as

multiple breaks in succession at the same location. Mice were habituated to the room for at least 1 hour before testing and then placed in the open field for 10 minutes. The enclosure was thoroughly cleaned with 95% ethanol and allowed to dry between each trial.

### 2.3. APP<sup>L/S</sup> mice

A well-characterized murine model of AD (Rockenstein et al., 2001), transgenic line 41 (C57BL/6) mice overexpressing human APP 751 containing the London (V717I) and Swedish (K670M/N671L) mutations, under the murine Thy1 promoter was kindly provided by Dr Eliezer Masliah at the University of California–San Diego and bred in our facilities. Female APP<sup>L/S</sup> mice and their wild-type (wt) littermates were randomized to either vehicle or LM11A-31 treatment. LM11A-31, 50 mg/kg/day dissolved in sterile water, was administered by oral gavage and vehicle-treated mice received an equivalent volume per weight of sterile water on the same schedule. Separate cohorts of mice were treated for each of two behavioral studies, the Y maze and Novel Object Recognition tests, as detailed below and in Supplementary Tables 1–3.

### 2.4. Novel object recognition test

Preliminary novel object recognition (NOR) testing showed onset of detectable deficits beginning at approximately 5 months of age. Beginning at 3 to 5 months of age, APP<sup>L/S</sup> mice and wt littermates were treated for 2.5 months before NOR testing at 5.5 to 7.5 months, as adapted from published protocols (Bevins and Besheer, 2006; Fernandez et al., 2007). Following test completion, mice were treated for 2 additional weeks before sacrifice (total treatment duration, ~3 months). Treatment group characteristics are shown in detail in Supplementary Table 2. Behavioral testing was observed in real time and recorded with an overhead video camera. On day 1, mice were placed with cage-mates for 15 minutes in the testing apparatus, a black acrylic enclosure (TAP Plastics) 48 cm long × 38 cm wide × 20 cm high. On day 2, each mouse was allowed to explore the box alone for 15 minutes. On day 3 (object exposure), each animal was placed in the box with two identical objects located in different corners of the box ~2 inches from the walls. The objects were either two small plastic red dice or two small plastic green blocks with distinctive indentations and contours. Baseline studies showed no innate preference between dice and blocks (data not shown). Mice were allowed to explore objects until 4 minutes of exploration had accrued; if 4 minutes of exploration was not reached, they were removed at 30 minutes. Object exploration was defined as contact with the object by the mouse's nose, forepaws, or whiskers. A 15-minute object recognition test was performed 24 hours later. Mice were placed back in the box with a "familiar" object (FO) that they had explored on day 3 and a novel object (NO). Objects were wiped clean with 95% ethanol after each exposure, and allowed to aerate for at least 15 minutes before the next exposure. The object role (novel vs. familiar) and position (left vs. right) were balanced within each experimental group. Two mice (1 APP<sup>L/S</sup> and 1 wt mouse treated with LM11A-31) that failed to achieve 30 seconds total exploration time in either the object exposure phase or the object recognition test were excluded from analysis. All testing and quantitation was conducted in a blinded fashion. Object recognition was quantified using a discrimination index (DI), defined as  $100 \times [(NO \text{ Time} - FO \text{ Time}) / (NO \text{ Time} + FO \text{ Time})]$  (Fernandez et al., 2007).

## 2.5. Y maze test

APP<sup>L/S</sup> mice exhibit deficits in the Y maze, a test of spatial working memory (Galvan et al., 2006). In preliminary Y maze studies, which followed the completion of NOR testing, it was found that genotype-related deficits in APP<sup>L/S</sup> mice were not detectable until 7 months of age; therefore, APP<sup>L/S</sup> mice and their wt littermates were treated with LM11A-31 or vehicle beginning at 4 to 6 months of age for approximately 3 months. Y maze testing was performed at 7 to 9 months of age. Treatment group characteristics are shown in detail in Supplementary Table 3. Each mouse was handled for ~1 minute daily for 14 days before testing. Immediately before testing, mice were habituated for at least 1 hour to the test environment, a small dimly lit room. Mice were placed in a white acrylic Y-shaped enclosure, with the 3 arms designated A, B, or C (arm A, ~8 × 5 × 3 inches; arms B and C, 6 × 5 × 3 inches; from TAP Plastics, Mountain View, CA). Sequential arm choices during an 8-minute exploration period by each mouse were recorded by a blinded observer. Percent spontaneous alternation was calculated based on the number of times that each arm choice differed from the previous two as  $100 \times [\text{number of spontaneous alternations}/(\text{total number of arm choices}-2)]$  (King and Arendash, 2002).

## 2.6. Immunohistochemistry

After 3 months of treatment, brains of mice tested for NOR (6–8 months of age at the time of sacrifice) and Y-maze (7–9 months at the time of sacrifice) were harvested for morphological and biochemical studies. For the entire NOR cohort and half of the Y-maze cohort, mice were perfused with heparinized saline, and brains were cut in the sagittal plane, 1 mm left of midline. The larger portion of the brain, containing the BFCNs, was post-fixed in 4% paraformaldehyde for 24 hours, then cryoprotected in 30% sucrose. Hippocampal and cortical tissues dissected from the smaller portion were immediately frozen on dry ice. For the remainder of the Y-maze cohort, the whole brain was collected as fresh frozen tissue. Fixed brain tissue was cut into 50- $\mu$ m coronal sections on a freezing microtome (Micron HM450, Thermo Scientific, Waltham, MA). Biotinylated APP antibody 8E5 was obtained from Elan Pharmaceuticals (South San Francisco, CA). Goat anti-ChAT antibody and biotinylated rabbit anti-goat secondary antibodies were obtained from Chemicon (Temecula, CA). Diaminobenzadine (DAB; Sigma, St Louis, MO) was used in combination with the Vectastain ABC detection kit (VectorLabs, Burlingame, CA). Biotinylated APP 8E5 antibody (1:1000) and goat anti-ChAT antibody (1:600) were used in conjunction with an ABC kit and DAB to visualize hippocampal (Games et al., 1995), BFCN and cortical dystrophic neurites (Knowles et al., 2009), respectively. Amyloid plaques were labeled with 1% thioflavin-S stain.

As detailed in the methods that follow (sections 2.7–2.10) and in Supplementary Table 1, the following studies made use of brain tissue from mice in the NOR cohort: BFCN stereology, BFCN neurite quantitation, quantitation of hippocampal dystrophic neurites, and enzyme-linked immunosorbent assay (ELISA). For studies of cholinergic cortical dystrophic neurites (section 2.9), brain tissue from mice in the Y maze and NOR groups was used in order to verify the protective effects of LM11A-31 in separate, independent cohorts, and to examine the effects of LM11A-31 in an age-stratified fashion.

## 2.7. BFCN stereology

Unbiased stereology was performed using the NOR cohort by an observer blind to experimental groups using Stereo Investigator software (MicroBrightField, Williston, VT). Under  $\times 5$  magnification, the basal forebrain was outlined. The basal forebrain was defined as the medial septum, vertical (VDB) and horizontal limbs of the diagonal band of Broca. The horizontal diagonal bands were included until they became discontinuous with the VDB. Every 4th section was analyzed (totaling 6–9 sections per animal) until the anterior commissure crossed the midline, approximately bregma 1.34 to 0.38 mm based on the mouse brain atlas of Franklin and Paxinos 3rd edition (Franklin and Paxinos, 2008). Average section thickness was measured before counting to determine guard zones and dissector height. We verified that ChAT antibody staining penetrated the full thickness of sections by examining z-stack images (taken at 0.5- $\mu\text{m}$  intervals) through representative sections from the basal forebrain region of each treatment group for uniformity of staining (Melvin and Sutherland, 2010) (Supplementary Fig. 2). Guard zones were set between 2 and 2.5  $\mu\text{m}$ , and dissector height was set between 6 and 11  $\mu\text{m}$ . Cells were counted in a  $75 \times 75\text{-}\mu\text{m}$  counting frame inside a  $100 \times 100\text{-}\mu\text{m}$  frame using a  $\times 40$  oil objective. Section thickness was measured at every 3rd counting site to maintain accurate measurements. To determine cell size, the Nucleator probe was used. Every other cell counted was measured with a 4-ray nucleator. Gundersen  $m = 1$  coefficient of error for cell counts was 0.05 or less. Cell size coefficient of error was 0.002 or less. Microscopy was performed on a Zeiss AxioImager M2 microscope (Carl Zeiss MicroImaging, Thornwood, NY).

## 2.8. Quantitation of BFCN neurites

Using the NOR cohort, the length of ChAT-immunostained neurites projecting directly from BFCNs was evaluated in the VDB, using methods adapted from previous work (Knowles et al., 2009). The VDB was defined by the area below the anterior commissure (anterior part) at the rostro-caudal level of the islands of Calleja and before the emergence of the horizontal diagonal band,  $\sim$ bregma 0.98 mm (Franklin and Paxinos, 2008); typically this criterion was met by only one section when every 8th section was processed. The length and area of ChAT-immunoreactive dendrites was assessed with NeuroLucida using an automated, unbiased scanning procedure (Meander Scan function) that allows areas of a user-defined contour to be viewed without overlap. In every 3rd meander scan, all neurons and the dendrites originating from them were manually traced while viewing tissue live with a  $\times 40$  objective and focusing up and down in the Z-plane. This method allowed accurate discrimination of the origins of neurites emanating from BFCNs. The Branched Structure Analysis function was used to compute the length, area and branching order of these neurites.

## 2.9. Quantitation of cholinergic dystrophic neurites in cortex

Brain sections from the NOR and Y-maze mouse cohorts were processed for ChAT immunostaining. Staining in the motor and primary somatosensory cortices (between  $\sim$ bregma 1.18 and 0.74 (Franklin and Paxinos, 2008)) was digitally imaged in 3 to 4 sections per animal while viewing with a  $\times 10$  objective (3–4 non-overlapping images per section; area of  $900 \times 670 \mu\text{m}^2$  for each image). Using NeuroLucida, the perimeters of the

clusters of ChAT-stained dystrophic neurites were manually traced, and mean cluster area was computed.

### 2.10. Quantitation of hippocampal dystrophic neurites

The following study used mice from the NOR cohort. Full-length APP accumulates in dystrophic neurites. Hence, APP immunostaining has been established as a marker for dystrophic neurites (Games et al., 1995; Knowles et al., 2009). APP-labeled dystrophic neurites were visualized using a Leica DM IRE2 light/fluorescence microscope. Percent area occupied by APP-stained dystrophic neurites in the central region of the hippocampus comprising the stratum lacunosum-moleculare and stratum radiatum was determined using ImageProPlus thresholding software (Mediacybernetics, Bethesda, MD). Sections were taken from the entire hippocampus at an inter-section interval of 400  $\mu\text{m}$  (every 8th section). One  $\times 10$  field covering the majority of the hippocampal area of each section was selected in a blinded fashion for analysis; between 3 and 7 sections were analyzed per mouse.

### 2.11. ELISA detection of A $\beta$

The following work used mice from the NOR cohort. A $\beta$  levels in brain extract were determined as previously described with minor modifications (McGowan et al., 2005). Antibodies 21F12 (A $\beta_{37-42}$ ) and biotinylated 3D6 (A $\beta_{1-5}$ ) were obtained from Elan. Hippocampal or cortical tissue was sonicated in RIPA buffer [50 mmol/L 1% Tris-HCl, 150 mmol/L NaCl, 200 mmol/L sodium orthovanadate, 1% NP40 detergent, 10% sodium deoxycholate, 10% SDS, 2X protease inhibitor cocktail (Roche Mini Tablet)] and centrifuged in a Beckman TL100 ultracentrifuge at 45,000 rpm, at 4  $^{\circ}\text{C}$  for 30 minutes. The supernatant, containing soluble A $\beta$  peptide, was retained. Plates coated with antibody 21F12 (5  $\mu\text{g}/\text{mL}$ ) were used to capture A $\beta_{x-42}$ ; the detection antibody was biotinylated 3D6 (2  $\mu\text{g}/\text{mL}$ ). Samples were then incubated with avidin-HRP (1:4000 dilution; Vector Laboratories) and developed using tetramethylbenzidine (TMB) as substrate (1-step Turbo TMB ELISA; Pierce Biotechnology). The reaction was terminated by addition of 2N sulfuric acid, and optical density read at 450 nm. Raw data were converted to ng/g wet tissue using a standard concentration curve of synthetic A $\beta$ .

### 2.12. NGF administration and hotplate testing

These analyses were conducted at UNC Chapel Hill Neuroscience Center with the permission of the Institutional Animal Care and Use Committee (UIACUC). Twenty 5-month-old female C57BL/6 mice were randomly assigned to 3 groups: vehicle (n = 4 mice); NGF (n = 8 mice); and LM11A-31 (n = 8 mice). Vehicle, NGF, and LM11A-31 were administered by intraperitoneal (IP) injection, because NGF would not be expected to achieve bioactive plasma levels if administered orally and the hyperalgesia effect of NGF had been previously established in mice using IP administration (2.5 mg/kg) (Della Seta et al., 1994). LM11A-31 was administered at a dose of 20 mg/kg with the goal of reaching a 1 hour plasma level similar to that reached by the 50 mg/kg OG dose used for efficacy studies ( $\sim 100$  ng/g; Fig. 1). Preliminary studies had demonstrated that an IP dose of 10 mg/kg resulted in a 1-hour plasma level of  $\sim 50$  ng/g and a linear dose-to-plasma level response; thus a dose of 20 mg/kg was selected for hotplate testing. Each mouse underwent pre-drug hotplate testing to ensure that there were no significant baseline differences between the



test groups. Mice were placed on the center of the Hotplate Analgesia Meter (Columbus Instrument, Columbus, OH), where the temperature was maintained at  $52^{\circ} \pm 0.1^{\circ}$  C. The latency time until first limb licking (either fore- or hind-limb) was recorded. 4 days later, each animal group was injected (IP) once with either vehicle (saline), NGF or LM11-31 and tested on the hot plate at 15, 30, 60, 180, and 360 minutes after injection. The latency to first licking (either fore- or hind-limb) was recorded by blinded observation.

### 2.13. Statistical analysis

Parametric tests were used as indicated in the figure legends. Data were determined to be normally distributed using the method of Kolmogorov and Smirnov. *p* values are indicated in figures or figure legends.

## 3. Results

### 3.1. LM11A-31 exhibits favorable brain bioavailability in the absence of overt toxicity

Before treating APP<sup>L/S</sup> mice with LM11A-31, we determined whether LM11A-31 crosses the blood brain barrier following oral administration. CNS bioavailability of LM11A-31 was initially assessed in CD-1 mice. A summary of mice used in this and all other analyses is provided in Supplementary Table 1. A single 50 mg/kg dose of LM11A-31 was administered by oral gavage and mice were sacrificed at various time points after dosing. As shown in Fig. 1A, peak brain concentration occurred approximately 30 minutes post dose at 262 ng/g, or approximately 1.08  $\mu\text{mol/L}$ ; this is above the dose range (100 nmol/L) that fully protected neurons against A $\beta$  in vitro (Yang et al., 2008). The brain half-life of LM11A-31 was 3 to 4 hours. Interestingly, beginning at the 1-hour time point, brain-to-plasma ratios were >1, a pharmacokinetic profile favorable for CNS targeting and raising the possibility of active CNS uptake. The brain-to-plasma ratio of atenolol was less than 5%, indicating no significant contamination of brain tissue extract by blood (data not shown).

To assess peak brain concentrations of LM11A-31 after chronic dosing in C57BL/6 mice, LM11A-31 was administered at 10, 50, or 100 mg/kg once per day by oral gavage to C57BL/6 mice for 2 weeks and mice were sacrificed 30 to 60 minutes after the last dose. Brain concentration in the 50 mg/kg/day group was 463.4 ng/g or approximately 1.9  $\mu\text{mol/L}$  (Fig. 1B), indicating that chronic daily dosing of a given dose (50 mg/kg) led to higher brain levels than after a single dose. Assuming a stable half-life of ~4 hours, the 30-to 60-minute level of 1.9  $\mu\text{mol/L}$  would likely lead to brain concentrations greater than or equal to 100 nmol/L for the majority of the 24-hour interdose interval. The brain-to-plasma ratio of LM11A-31 in the 50 mg/kg treatment group was found to be  $3.1 \pm 0.9$ . To screen for toxic effects, mice treated with LM11A-31 at 50 mg/kg once daily for 9 days were tested in an open field, revealing no behavioral differences (Fig. 1C and D). The weights of these mice were monitored during the 2-week dosing period, showing no differences between treatment groups (Fig. 1E).

### 3.2. Oral administration of LM11A-31 to APP<sup>L/S</sup> mice prevents deficits in novel object recognition in APP<sup>L/S</sup> mice

Given our previous finding of reduced neuritic degeneration in APP<sup>L/S</sup> mice expressing mutant p75<sup>NTR</sup> (p75<sup>NTR</sup> exon III  $-/-$   $\times$  APP<sup>L/S</sup>) (Knowles et al., 2009), we selected the same APP<sup>L/S</sup> mouse model (Rockenstein et al., 2001) to determine whether oral administration of LM11A-31 would reduce neurite degeneration and, in addition, behavioral deficits. In NOR testing, wt mice spent more time exploring a novel object relative to a familiar object, whereas vehicle-treated APP<sup>L/S</sup> mice did not recognize objects to which they had been previously exposed (Fig. 2A). Loss of object recognition in APP<sup>L/S</sup> mice was prevented by LM11A-31 treatment (Fig. 2A). No significant differences in total object exploration time were observed across treatment groups (Fig. 2B), although there was a non-significant reduction in total exploration time related to genotype (Fig. 2B). Treatment was continued for an additional 2 weeks before sacrifice.

### 3.3. LM11A-31 prevents deficits in spatial working memory

To further evaluate the range of treatment effects on behavioral deficits, we investigated the effects of LM11A-31 on spatial working memory using the Y maze. Vehicle- and LM11A-31-treated wt mice exhibited no difference in the rate of maze arm entries without repetition (Fig. 2C), with spontaneous alternation of Y-arm choice occurring approximately 65% of the time, consistent with previously reported findings (Galvan et al., 2006). The performance of vehicle-treated APP<sup>L/S</sup> mice approached that of chance performance (50%, indicated by a dotted line in Fig. 2C), suggesting nearly complete impairment of spatial working memory. Treatment with LM11A-31 significantly improved test performance such that it was indistinguishable from that of wt mice. The total number of arm entries did not vary significantly between groups (Fig. 2D). A few days after Y maze testing was complete, mice were sacrificed, and tissue was processed for histology.

### 3.4. BFCN size and number are not affected in APP<sup>L/S</sup> mice treated with LM11A-31

We previously found that the number and size of BFCNs are unaffected in APP<sup>L/S</sup> mice in an age range similar to that used in this study (Knowles et al., 2009). However, we reasoned that LM11A-31 might enhance BFCN structure (such as increased neuronal size) even in the absence of a pre-existing deficit, thereby contributing to enhanced cognitive performance. Also of concern was the possibility that a small molecule ligand targeting p75<sup>NTR</sup> but not TrkA might have a deleterious effect on BFCNs (such as atrophy). Consistent with previous results, unbiased stereological analysis of ChAT-immunostained brain sections from mice tested for NOR revealed no impact of the transgene on BFCNs. Moreover, LM11A-31 administration had no effect on BFCN number (Fig. 3A) or size (Fig. 3B).

### 3.5. LM11A-31 prevents BFCN neurite degeneration in APP<sup>L/S</sup> mice

Our prior work showed that the morphological status of BFCN projection fibers is modulated by p75<sup>NTR</sup> (Yeo et al., 1997) and that neuritic atrophy of BFCNs was prominent in APP<sup>L/S</sup> mice and absent in APP<sup>L/S</sup> mice expressing mutant p75<sup>NTR</sup> (Knowles et al., 2009). We used manual NeuroLucida neurite tracing to analyze neurites projecting directly from BFCNs in the VDB (Fig. 4A), which contains a proportionately larger projection to

the cortex and hippocampus than the medial septum (Lamour et al., 1982; Mesulam et al., 1983). The mean number of neurons examined per mouse was  $63 \pm 17$  (SD). Vehicle-treated APP<sup>L/S</sup> mice exhibited atrophic cholinergic neurites (Fig. 4A), similar to previous work (Knowles et al., 2009). Mean dendritic length and area in vehicle-treated APP<sup>L/S</sup> mice were significantly reduced compared to vehicle-treated wt mice (Fig. 4B and C). Similarly, the mean length of 2nd-order branches of ChAT-stained dendrites was significantly reduced in vehicle-treated APP<sup>L/S</sup> compared to wt mice (Fig. 4D). Treatment of APP<sup>L/S</sup> mice with LM11A-31 significantly prevented this loss of neurite length and branching (Fig. 4B and D), and there was a statistically nonsignificant increase in neurite area with treatment (95% confidence interval -11.6% to 69.2%) (Fig. 4C).

### 3.6. LM11A-31 reduces cholinergic dystrophic neurites in cortex of APP<sup>L/S</sup> mice

Neurons of the basal forebrain provide the main cholinergic innervation to the cortex (Mesulam et al., 1983) and cholinergic fibers often become progressively dystrophic in the vicinity of amyloid plaques (German et al., 2003; Perez et al., 2007), potentially contributing to functional impairment (Knowles et al., 1999). Given previous work demonstrating increasing cortical neuritic dystrophy with age (Perez et al., 2007), we examined the effects of LM11A-31 treatment on cortical cholinergic dystrophic neurites separately in the NOR cohort (collected at a mean age of ~7 months) and the older Y-maze cohort (collected at a mean age of ~8 months). In both groups, dystrophic ChAT-stained neurites were absent in the cortex of wt mice (not shown) but were readily visible as clusters of dilated neuritic processes primarily surrounding plaques in vehicle-treated APP<sup>L/S</sup> mice, and there was an apparent decrease in cluster size with LM11A-31 treatment (Fig. 5A). As shown in Fig. 5B, quantitative analysis showed that the mean dystrophic neurite cluster area was higher in the 8-month group and LM11A-31 reduced the mean cluster area, in both groups (Fig. 5B).

### 3.7. LM11A-31 prevents hippocampal neurite degeneration in APP<sup>L/S</sup> mice

In our previous study (Knowles et al., 2009), hippocampal dystrophic neurites identified with APP antibody 8E5 (an established marker of dystrophic neurites that does not label A $\beta$  or amyloid deposits) were diminished in APP<sup>L/S</sup> mice expressing mutant p75<sup>NTR</sup>. We examined hippocampal neuritic dystrophy in APP<sup>L/S</sup> mice used in the NOR cohort. In vehicle-treated APP<sup>L/S</sup> mice, neuritic dystrophy was prominent, particularly in the vicinity of Thioflavin S-labeled plaques (Fig. 6A). Treatment of APP<sup>L/S</sup> mice with LM11A-31 was associated with a markedly diminished degree of neuritic dystrophy, although qualitatively plaque size, morphology, and density appeared to be unaffected (Fig. 6A). Quantitative studies demonstrated that the area occupied by APP-immunolabeled dystrophic neurites in the hippocampus was decreased by approximately 50% in LM11A-31-treated APP<sup>L/S</sup> mice (Fig. 6B).

### 3.8. Neuroprotective effects of LM11A-31 are not attributable to lower A $\beta$ (1–42) levels

Plaque size appeared comparable between APP<sup>L/S</sup> mice treated with vehicle and LM11A-31 (Fig. 6A); however, Thioflavin S stains primarily fibrillar forms of A $\beta$ , and may also stain some dystrophic neurites (Murray et al., 2011). Therefore, to more accurately determine whether the beneficial effects of LM11A-31 were related to decreased brain amyloid levels, we quantified soluble A $\beta$ (1–42) in brains of APP<sup>L/S</sup> mice from the NOR cohort treated

with vehicle or LM11A-31 using ELISA. Hippocampal and cortical A $\beta$ (1–42) levels in vehicle-treated mice were not different from levels in LM11A-31–treated animals (Fig. 6C and D). Thus, the mechanism by which LM11A-31 exerts beneficial effects on behavior and morphology is unlikely to involve a decrease in A $\beta$  levels.

### 3.9. LM11A-31 does not induce hyperalgesia

In human studies, intrathecal administration of NGF for the treatment of AD was limited by severe pain in treated subjects (Eriksdotter Jonhagen et al., 1998). In rodent studies, peripheral NGF administration has been shown to induce weight loss and pain phenomena with heat hyperalgesia being particularly well characterized (Della Seta et al., 1994; Hao et al., 2000). To determine whether LM11A-31 might also have this effect, vehicle, NGF, or LM11A-31 was administered to wt mice in a single IP injection followed by heat hyperalgesia testing using a protocol previously established in NGF studies (Della Seta et al., 1994). As described in the Methods, LM11A-31 was administered at a dose providing high plasma concentrations similar to those occurring with the oral gavage dose. Mice treated with vehicle showed a heat response latency of approximately 20 seconds, whereas those treated with NGF developed significantly decreased latencies within 30 minutes after treatment, consistent with NGF induction of heat hyperalgesia (Fig. 7) as in previous studies (Della Seta et al., 1994). In marked contrast, the response to LM11A-31 was indistinguishable from that of vehicle, indicating an absence of LM11A-31 induced heat hyperalgesia.

## 4. Discussion

The present studies demonstrate that oral administration of LM11A-31 to APP<sup>L/S</sup> mice leads to therapeutic brain levels and achieves the designated endpoints of prevention of NOR and Y-maze behavioral deficits, accompanied by decreased BFCN, hippocampal and cortical neurite degeneration. At the same time, LM11A-31 did not affect amyloid levels or cause weight loss and lowered pain threshold, two effects that had limited the application of NGF in clinical studies.

The present findings lend substantial support to the hypothesis that p75<sup>NTR</sup> enables and/or contributes to A $\beta$ -induced degeneration in AD animal models (Knowles et al., 2009; Sotthibundhu et al., 2008). Previous in vitro studies showed that LM11A-31 activates survival signaling (AKT and NF $\kappa$ B) in a p75<sup>NTR</sup>-dependent fashion (Massa et al., 2006), that it inhibits A $\beta$ -induced degenerative signaling (including GSK3 $\beta$ , calpain, cdk5, and c-jun activation) as well as as A $\beta$ -induced reduction of AKT and CREB signaling (Yang et al., 2008). Together with those findings, the present work indicates that LM11A-31 is capable of acting through p75<sup>NTR</sup> to prevent progression of AD-related pathology and behavioral deficits in vivo. Details of in vivo signaling pathways downstream from p75<sup>NTR</sup> through which LM11A-31 achieves these effects will be further elucidated in future studies. Another remaining question is whether LM11A-31 can reverse neuritic dystrophy and other degenerative processes once these changes are in more advanced stages. Ongoing studies in our laboratory are addressing this question using mice in older age groups.

As is the case for any in vivo drug application, the possibility of other targets remains. The standard approach for evaluating target specificity is to determine whether removal of the target, generally through knock-out models, abolishes the therapeutic effect. A challenge in the case of p75<sup>NTR</sup> is that its removal in the AD mouse model used here leads to the therapeutic effect of reduced A $\beta$ -associated degeneration (Knowles et al., 2009). To date, we have confirmed that LM11A-31 does not bind to or have any effect on Trk receptor signaling; it does not promote survival or AKT activation in p75<sup>NTR</sup>  $-/-$  neurons; and LM11A-31 is functionally entirely blocked by antibodies directed to the extracellular domain of p75<sup>NTR</sup> (Massa et al., 2006). Screening of a CEREP panel of receptors used to identify alternative drug targets was negative (Yang et al., 2008). Nevertheless, future studies will continue to evaluate possible off-target mechanisms, as occurs with already established drugs.

LM11A-31 has also been administered to mice after contusion spinal cord injury (Tep et al., 2013). In this model, injury induces increased levels of proNGF, which binds to p75<sup>NTR</sup>, leading to oligodendrocyte JNK3 activation, oligodendrocyte death, and spinal cord demyelination. LM11A-31 inhibited proNGF interaction with p75<sup>NTR</sup>, reduced JNK3 activation, reduced oligodendrocyte death, reduced demyelination, and improved functional outcome. In p75<sup>NTR</sup>  $-/-$  mice, LM11A-31 failed to inhibit injury-induced JNK3 activation, further supporting a role for p75<sup>NTR</sup> in mediating its therapeutic effect.

An important question in the AD model is whether similar therapeutic effects of LM11A-31 could be achieved with a shorter treatment interval. In this initial study, we chose a 3-month treatment interval based on the assumption that A $\beta$  accumulation and the resulting structural degeneration, particularly of BFCN populations, occur over a period of weeks to months in APP<sup>L/S</sup> mice. However, cognitive impairment in AD also involves rapid and sometimes transient alterations in synaptic function superimposed on chronic neurodegeneration. Furthermore, neurotrophin signaling through p75<sup>NTR</sup> has been reported to regulate hippocampal synaptic function, specifically long-term depression (Rosch et al., 2005; Woo et al., 2005). If LM11A-31 were positively affecting synaptic function, effects might be seen after shorter treatment intervals. We previously found that mouse hippocampal slices treated with oligomeric A $\beta$  exhibit deficits in LTP, which were corrected by administration of LM11A-31 (Yang et al., 2008). Although the present study focused on the long-term structural effects of LM11A-31, ongoing studies in our laboratory are examining potential acute effects of p75<sup>NTR</sup> small molecule ligands.

A key limitation of the application of NGF in AD has been the need to target certain neuronal populations (such as BFCNs) while avoiding NGF-induced toxicity in other populations. Indeed, a significant body of work has targeted NGF expression to discrete anatomic areas such as the basal forebrain, using ex vivo and in vivo gene delivery (Tuszynski, 2007), including a Phase I human clinical trial for the treatment of AD (Tuszynski et al., 2005). Regional specificity may not be as critical in the administration of LM11A-31 given that this and previous work have demonstrated that LM11A-31 induces pro-survival signaling through p75<sup>NTR</sup> but not Trk (Massa et al., 2006) and, unlike NGF, does not induce weight loss or hyperalgesia. Moreover, the lack of cognitive impairment in LM11A-31 treated wt animals and the improved cognitive performance in LM11A-31-

treated APP<sup>L/S</sup> mice argue against neurotoxic effects. As a ligand of the p75<sup>NTR</sup> receptor with a signaling profile distinct from that of NGF, LM11A-31 and other small molecules in its class represent a therapeutic strategy that is separate from, and not mutually exclusive with, targeted gene delivery of NGF.

Of note, the 50-mg/kg dose of LM11A-31 used in the present murine study predicts a human equivalent dose of approximately 280 mg using standard body surface area conversion, indicating a dose range that is quite amenable for drug development. Future studies will further establish effective dose–response ranges.

The present findings support an important role for p75<sup>NTR</sup> in AD-related mechanisms, and provide the first report of a small molecule targeted to p75<sup>NTR</sup> preventing AD-related cognitive deficits and neurodegeneration. This work provides validation for the further development of p75<sup>NTR</sup> ligands as a novel class of target-specific neuroprotective compounds for the treatment of AD.

## Supplementary Material

Refer to Web version on PubMed Central for supplementary material.

## Acknowledgements

This project was supported by funding from NINDS F30 NA051971 (J.K.K.), NIA UO1 AG032225 (F.M.L.), NS049442 (O.A.), the Alzheimer's Drug Discovery Foundation (F.M.L.), Alzheimer's Association (F.M.L.), the Eastern Chapter of the North Carolina Alzheimer's Association (F.M.L.), the Jean Perkins Foundation (F.M.L.), and the Horngren Family Alzheimer's Research Fund (F.M.L.), the Richard M. Lucas Foundation (F.M.L.) and the Veterans Administration (S.M.M. and T.W.C.). The authors thank Chihiro Ishikawa and Mary Wilson for their assistance in the execution of this work.

## References

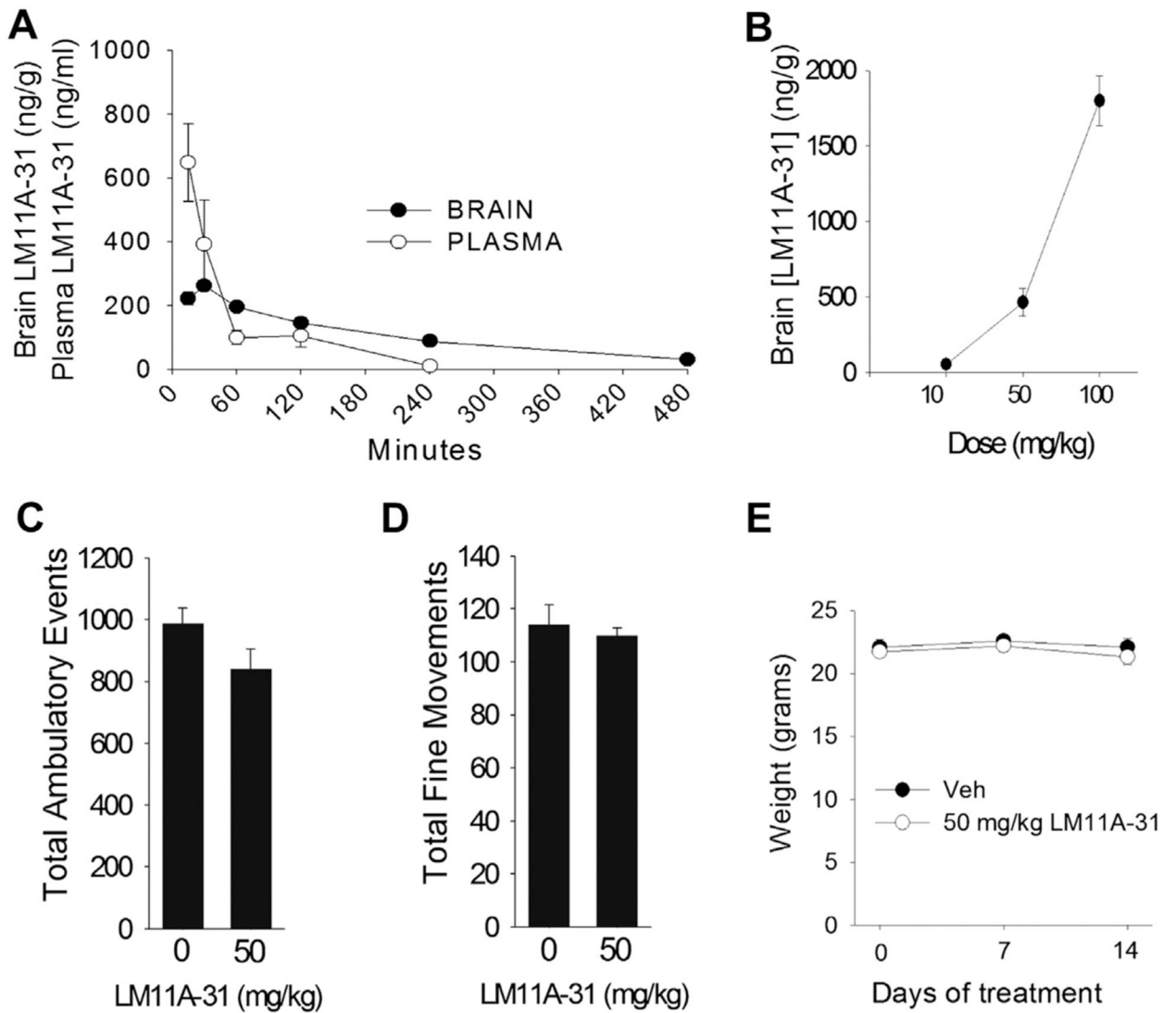
- Barker PA, 2004. p75<sup>NTR</sup> is positively promiscuous: novel partners and new insights. *Neuron* 42, 529–533. [PubMed: 15157416]
- Bergmann I, Reiter R, Toyka KV, Koltzenburg M, 1998. Nerve growth factor evokes hyperalgesia in mice lacking the low-affinity neurotrophin receptor p75. *Neurosci. Lett* 255, 87–90. [PubMed: 9835221]
- Bevins RA, Besheer J, 2006. Object recognition in rats and mice: a one-trial non-matching-to-sample learning task to study 'recognition memory'. *Nat. Protoc* 1, 1306–1311. [PubMed: 17406415]
- Bruns MB, Miller MW, 2007. Neurotrophin ligand-receptor systems in somatosensory cortex of adult rat are affected by repeated episodes of ethanol. *Exp. Neurol* 204, 680–692. [PubMed: 17320080]
- Chakravarthy B, Gaudet C, Menard M, Atkinson T, Brown L, Laferla FM, Armato U, Whitfield J, 2010. Amyloid-beta peptides stimulate the expression of the p75(NTR) neurotrophin receptor in SHSY5Y human neuroblastoma cells and AD transgenic mice. *J. Alzheimers Dis* 19, 915–925. [PubMed: 20157247]
- Chakravarthy B, Menard M, Ito S, Gaudet C, Dal Pra I, Armato U, Whitfield J, 2012. Hippocampal membrane-associated p75<sup>NTR</sup> levels are increased in Alzheimer's disease. *J. Alzheimers Dis* 30, 675–684. [PubMed: 22451321]
- Coulson EJ, 2006. Does the p75 neurotrophin receptor mediate Abeta-induced toxicity in Alzheimer's disease? *J. Neurochem* 98, 654–660. [PubMed: 16893414]
- Dechant G, Barde YA, 2002. The neurotrophin receptor p75(NTR): novel functions and implications for diseases of the nervous system. *Nat. Neurosci* 5, 1131–1136. [PubMed: 12404007]

- Della Seta D, de Acetis L, Aloe L, Alleva E, 1994. NGF effects on hot plate behaviors in mice. *Pharmacol. Biochem. Behav* 49, 701–705. [PubMed: 7862726]
- Diarra A, Geetha T, Potter P, Babu JR, 2009. Signaling of the neurotrophin receptor p75 in relation to Alzheimer's disease. *Biochem. Biophys. Res. Commun* 390, 352–356. [PubMed: 19818333]
- Dougherty KD, Milner TA, 1999. p75NTR immunoreactivity in the rat dentate gyrus is mostly within presynaptic profiles but is also found in some astrocytic and postsynaptic profiles. *J. Comp. Neurol* 407, 77–91. [PubMed: 10213189]
- Eriksdotter Jonhagen M, Nordberg A, Amberla K, Backman L, Ebendal T, Meyerson B, Olson L, Seiger, Shigeta M, Theodorsson E, Viitanen M, Winblad B, Wahlund LO, 1998. Intracerebroventricular infusion of nerve growth factor in three patients with Alzheimer's disease. *Dement. Geriatr. Cogn. Disord* 9, 246–257. [PubMed: 9701676]
- Fernandez F, Morishita W, Zuniga E, Nguyen J, Blank M, Malenka RC, Garner CC, 2007. Pharmacotherapy for cognitive impairment in a mouse model of Down syndrome. *Nat. Neurosci* 10, 411–413. [PubMed: 17322876]
- Franklin KBJ, Paxinos G, 2008. *The Mouse Brain in Stereotaxic Coordinates*. Elsevier Science, Amsterdam.
- Friedman WJ, 2000. Neurotrophins induce death of hippocampal neurons via the p75 receptor. *J. Neurosci* 20, 6340–6346. [PubMed: 10964939]
- Galvan V, Gorostiza OF, Banwait S, Ataie M, Logvinova AV, Sitaraman S, Carlson E, Sagi SA, Chevallier N, Jin K, Greenberg DA, Bredesen DE, 2006. Reversal of Alzheimer's-like pathology and behavior in human APP transgenic mice by mutation of Asp664. *Proc. Natl. Acad. Sci. U. S. A* 103, 7130–7135. [PubMed: 16641106]
- Games D, Adams D, Alessandrini R, Barbour R, Berthelette P, Blackwell C, Carr T, Clemens J, Donaldson T, Gillespie F, Guido T, Hagopian S, Johnson-Wood K, Khan K, Lee M, Leibowitz P, Lieberburg I, Little S, Masliah E, McConlogue L, Montoya-Zavala M, Mucke L, Paganini L, Penniman E, Power M, Schenk D, Seubert P, Snyder B, Soriano F, Tan H, Vitale J, Wadsworth S, Wolozin B, Zhao J, 1995. Alzheimer-type neuropathology in transgenic mice overexpressing V717F beta-amyloid precursor protein. *Nature* 373, 523–527. [PubMed: 7845465]
- German DC, Yazdani U, Speciale SG, Pasbakhsh P, Games D, Liang CL, 2003. Cholinergic neuropathology in a mouse model of Alzheimer's disease. *J. Comp. Neurol* 462, 371–381. [PubMed: 12811807]
- Ginsberg SD, Che S, Wu J, Counts SE, Mufson EJ, 2006. Down regulation of trk but not p75NTR gene expression in single cholinergic basal forebrain neurons mark the progression of Alzheimer's disease. *J. Neurochem* 97, 475–487. [PubMed: 16539663]
- Greferath U, Bennie A, Kourakis A, Bartlett PF, Murphy M, Barrett GL, 2000. Enlarged cholinergic forebrain neurons and improved spatial learning in p75 knockout mice. *Eur. J. Neurosci* 12, 885–893. [PubMed: 10762318]
- Hao J, Ebendal T, Xu X, Wiesenfeld-Hallin Z, Eriksdotter Jonhagen M, 2000. Intracerebroventricular infusion of nerve growth factor induces pain-like response in rats. *Neurosci. Lett* 286, 208–212. [PubMed: 10832021]
- Hefti F, Weiner WJ, 1986. Nerve growth factor and Alzheimer's disease. *Ann. Neurol* 20, 275–281. [PubMed: 3532929]
- Ibanez CF, Simi A, 2012. p75 Neurotrophin receptor signaling in nervous system injury and degeneration: paradox and opportunity. *Trends Neurosci.* 35, 431–440. [PubMed: 22503537]
- Jacobs JS, Miller MW, 1999. Expression of nerve growth factor, p75, and the high affinity neurotrophin receptors in the adult rat trigeminal system: evidence for multiple trophic support systems. *J. Neurocytol* 28, 571–595. [PubMed: 10800206]
- James SE, Burden H, Burgess R, Xie Y, Yang T, Massa SM, Longo FM, Lu Q, 2008. Anti-cancer drug induced neurotoxicity and identification of Rho pathway signaling modulators as potential neuroprotectants. *Neurotoxicology.* 29, 605–612. [PubMed: 18539332]
- King DL, Arendash GW, 2002. Maintained synaptophysin immunoreactivity in Tg2576 transgenic mice during aging: correlations with cognitive impairment. *Brain Res.* 926, 58–68. [PubMed: 11814407]

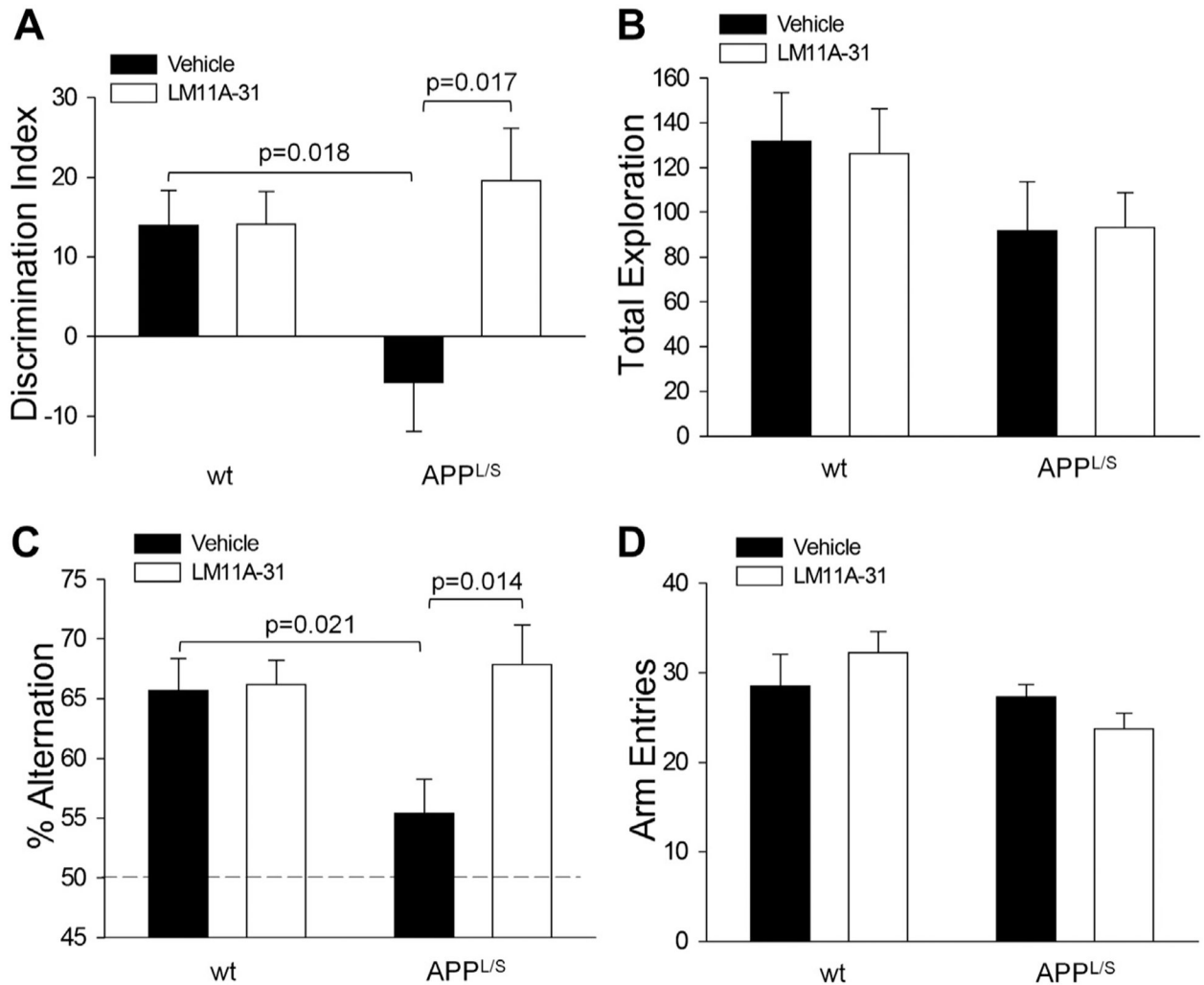
- Knowles JK, Rajadas J, Nguyen TV, Yang T, LeMieux MC, Vander Griend L, Ishikawa C, Massa SM, Wyss-Coray T, Longo FM, 2009. The p75 neurotrophin receptor promotes amyloid-beta(1–42)-induced neuritic dystrophy in vitro and in vivo. *J. Neurosci* 29, 10627–10637. [PubMed: 19710315]
- Knowles RB, Wyart C, Buldyrev SV, Cruz L, Urbanc B, Hasselmo ME, Stanley HE, Hyman BT, 1999. Plaque-induced neurite abnormalities: implications for disruption of neural networks in Alzheimer's disease. *Proc. Natl. Acad. Sci. U. S. A* 96, 5274–5279. [PubMed: 10220456]
- Kromer LF, 1987. Nerve growth factor treatment after brain injury prevents neuronal death. *Science* 235, 214–216. [PubMed: 3798108]
- Lamour Y, Dutar P, Jobert A, 1982. Topographic organization of basal forebrain neurons projecting to the rat cerebral cortex. *Neurosci. Lett* 34, 117–122. [PubMed: 6306515]
- Lee R, Kermani P, Teng KK, Hempstead BL, 2001. Regulation of cell survival by secreted proneurotrophins. *Science* 294, 1945–1948. [PubMed: 11729324]
- Longo FM, Massa SM, 2004. Neuroprotective strategies in Alzheimer's disease. *NeuroRx* 1, 117–127. [PubMed: 15717012]
- Longo FM, Massa SM, 2005. Neurotrophin receptor-based strategies for Alzheimer's disease. *Curr. Alzheimer Res* 2, 167–169. [PubMed: 15974914]
- Massa SM, Xie Y, Yang T, Harrington AW, Kim ML, Yoon SO, Kraemer R, Moore LA, Hempstead BL, Longo FM, 2006. Small, nonpeptide p75NTR ligands induce survival signaling and inhibit proNGF-induced death. *J. Neurosci* 26, 5288–5300. [PubMed: 16707781]
- McGowan E, Pickford F, Kim J, Onstead L, Eriksen J, Yu C, Skipper L, Murphy MP, Beard J, Das P, Jansen K, Delucia M, Lin WL, Dolios G, Wang R, Eckman CB, Dickson DW, Hutton M, Hardy J, Golde T, 2005. Abeta42 is essential for parenchymal and vascular amyloid deposition in mice. *Neuron* 47, 191–199. [PubMed: 16039562]
- Melvin NR, Sutherland RJ, 2010. Quantitative caveats of standard immunohistochemical procedures: implications for optical disector-based designs. *J Histochem. Cytochem* 58, 577–584. [PubMed: 19995945]
- Mesulam MM, Mufson EJ, Wainer BH, Levey AI, 1983. Central cholinergic pathways in the rat: an overview based on an alternative nomenclature (Ch1-Ch6). *Neuroscience* 10, 1185–1201. [PubMed: 6320048]
- Mufson EJ, Counts SE, Perez SE, Ginsberg SD, 2008. Cholinergic system during the progression of Alzheimer's disease: therapeutic implications. *Expert Rev. Neurother* 8, 1703–1718. [PubMed: 18986241]
- Mufson EJ, Kordower JH, 1992. Cortical neurons express nerve growth factor receptors in advanced age and Alzheimer disease. *Proc. Natl. Acad. Sci. U. S. A* 89, 569–573. [PubMed: 1309947]
- Mufson EJ, Lavine N, Jaffar S, Kordower JH, Quirion R, Saragovi HU, 1997. Reduction in p140-TrkA receptor protein within the nucleus basalis and cortex in Alzheimer's disease. *Exp. Neurol* 146, 91–103. [PubMed: 9225742]
- Mufson EJ, Li JM, Sobreviela T, Kordower JH, 1996. Decreased trkA gene expression within basal forebrain neurons in Alzheimer's disease. *Neuroreport* 8, 25–29. [PubMed: 9051746]
- Murray ME, Graff-Radford NR, Ross OA, Petersen RC, Duara R, Dickson DW, 2011. Neuropathologically defined subtypes of Alzheimer's disease with distinct clinical characteristics: a retrospective study. *Lancet Neurol.* 10, 785–796. [PubMed: 21802369]
- Naumann T, Casademunt E, Hollerbach E, Hofmann J, Dechant G, Frotscher M, Barde YA, 2002. Complete deletion of the neurotrophin receptor p75NTR leads to long-lasting increases in the number of basal forebrain cholinergic neurons. *J. Neurosci* 22, 2409–2418. [PubMed: 11923404]
- Perez SE, Dar S, Ikonovic MD, DeKosky ST, Mufson EJ, 2007. Cholinergic forebrain degeneration in the APP<sup>swe</sup>/PS1<sup>DeltaE9</sup> transgenic mouse. *Neurobiol. Dis* 28, 3–15. [PubMed: 17662610]
- Perini G, Della-Bianca V, Politi V, Della Valle G, Dal-Pra I, Rossi F, Armato U, 2002. Role of p75 neurotrophin receptor in the neurotoxicity by beta-amyloid peptides and synergistic effect of inflammatory cytokines. *J. Exp. Med* 195, 907–918. [PubMed: 11927634]
- Rabizadeh S, Bitler CM, Butcher LL, Bredesen DE, 1994. Expression of the low-affinity nerve growth factor receptor enhances beta-amyloid peptide toxicity. *Proc. Natl. Acad. Sci. U. S. A* 91, 10703–10706. [PubMed: 7938014]



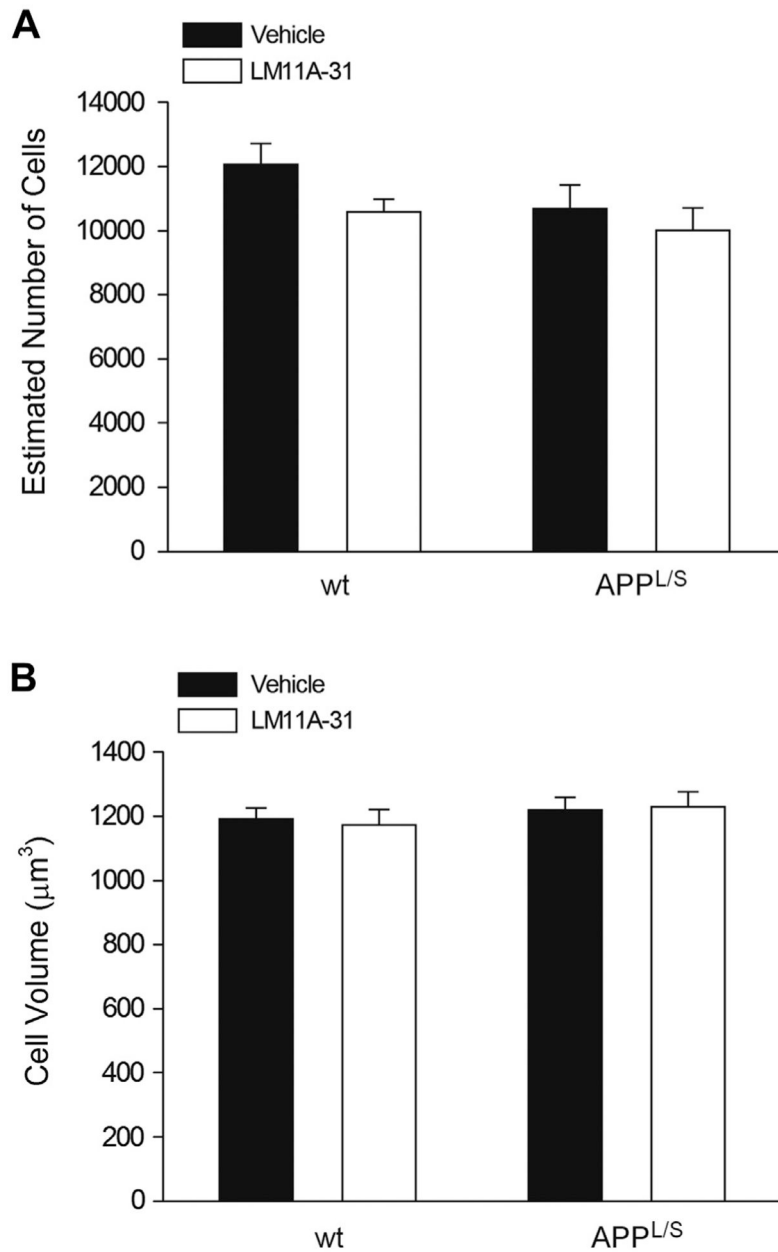
- Rockenstein E, Mallory M, Mante M, Sisk A, Masliha E, 2001. Early formation of mature amyloid-beta protein deposits in a mutant APP transgenic model depends on levels of Abeta(1–42). *J. Neurosci. Res* 66, 573–582. [PubMed: 11746377]
- Rosch H, Schweigreiter R, Bonhoeffer T, Barde YA, Korte M, 2005. The neurotrophin receptor p75NTR modulates long-term depression and regulates the expression of AMPA receptor subunits in the hippocampus. *Proc. Natl. Acad. Sci. U. S. A* 102, 7362–7367. [PubMed: 15883381]
- Roux PP, Barker PA, 2002. Neurotrophin signaling through the p75 neurotrophin receptor. *Prog. Neurobiol* 67, 203–233. [PubMed: 12169297]
- Schliebs R, Arendt T, 2011. The cholinergic system in aging and neuronal degeneration. *Behav. Brain Res* 221, 555–563. [PubMed: 21145918]
- Sofroniew MV, Howe CL, Mobley WC, 2001. Nerve growth factor signaling, neuroprotection, and neural repair. *Annu. Rev. Neurosci* 24, 1217–1281. [PubMed: 11520933]
- Sothibundhu A, Sykes AM, Fox B, Underwood CK, Thangnipon W, Coulson EJ, 2008. Beta-amyloid(1–42) induces neuronal death through the p75 neurotrophin receptor. *J. Neurosci* 28, 3941–3946. [PubMed: 18400893]
- Teng KK, Felice S, Kim T, Hempstead BL, 2010. Understanding proneurotrophin actions: recent advances and challenges. *Dev. Neurobiol* 70, 350–359. [PubMed: 20186707]
- Tep C, Lim TH, Ko PO, Getahun S, Ryu JC, Goettl VM, Massa SM, Basso M, Longo FM, Yoon SO, 2013. Oral administration of a small molecule targeted to block proNGF binding to p75 promotes myelin sparing and functional recovery after spinal cord injury. *J. Neurosci* 33, 397–410. [PubMed: 23303920]
- Tuszynski MH, 2007. Nerve growth factor gene therapy in Alzheimer disease. *Alzheimer Dis. Assoc. Disord* 21, 179–189. [PubMed: 17545746]
- Tuszynski MH, Thal L, Pay M, Salmon DP, U HS, Bakay R, Patel P, Blesch A, Vahlsing HL, Ho G, Tong G, Potkin SG, Fallon J, Hansen L, Mufson EJ, Kordower JH, Gall C, Conner J, 2005. A phase 1 clinical trial of nerve growth factor gene therapy for Alzheimer disease. *Nat. Med* 11, 551–555. [PubMed: 15852017]
- Tuszynski MH, U HS, Amaral DG, Gage FH, 1990. Nerve growth factor infusion in the primate brain reduces lesion-induced cholinergic neuronal degeneration. *J. Neurosci* 10, 3604–3614. [PubMed: 2230949]
- Ugolini G, Marinelli S, Covaceuszach S, Cattaneo A, Pavone F, 2007. The function neutralizing anti-TrkA antibody MNAC13 reduces inflammatory and neuropathic pain. *Proc. Natl. Acad. Sci. U. S. A* 104, 2985–2990. [PubMed: 17301229]
- Underwood CK, Coulson EJ, 2008. The p75 neurotrophin receptor. *Int. J. Biochem. Cell Biol* 40, 1664–1668. [PubMed: 17681869]
- Vana L, Kanaan NM, Ugwu IC, Wu J, Mufson EJ, Binder LI, 2011. Progression of tau pathology in cholinergic basal forebrain neurons in mild cognitive impairment and Alzheimer's disease. *Am. J. Pathol* 179, 2533–2550. [PubMed: 21945902]
- Williams LR, Varon S, Peterson GM, Wictorin K, Fischer W, Bjorklund A, Gage FH, 1986. Continuous infusion of nerve growth factor prevents basal forebrain neuronal death after fimbria fornix transection. *Proc. Natl. Acad. Sci. U. S. A* 83, 9231–9235. [PubMed: 3466184]
- Woo NH, Teng HK, Siao CJ, Chiaruttini C, Pang PT, Milner TA, Hempstead BL, Lu B, 2005. Activation of p75NTR by proBDNF facilitates hippocampal long-term depression. *Nat. Neurosci* 8, 1069–1077. [PubMed: 16025106]
- Yaar M, Zhai S, Pilch PF, Doyle SM, Eisenhauer PB, Fine RE, Gilchrist BA, 1997. Binding of beta-amyloid to the p75 neurotrophin receptor induces apoptosis. A possible mechanism for Alzheimer's disease. *J. Clin. Invest* 100, 2333–2340. [PubMed: 9410912]
- Yang T, Knowles JK, Lu Q, Zhang H, Arancio O, Moore LA, Chang T, Wang Q, Andreasson K, Rajadas J, Fuller GG, Xie Y, Massa SM, Longo FM, 2008. Small molecule, non-peptide p75 ligands inhibit Abeta-induced neurodegeneration and synaptic impairment. *PLoS ONE* 3, e3604. [PubMed: 18978948]
- Yeo TT, Chua-Couzens J, Butcher LL, Bredesen DE, Cooper JD, Valletta JS, Mobley WC, Longo FM, 1997. Absence of p75NTR causes increased basal forebrain cholinergic neuron size, choline acetyltransferase activity, and target innervation. *J. Neurosci* 17, 7594–7605. [PubMed: 9315882]



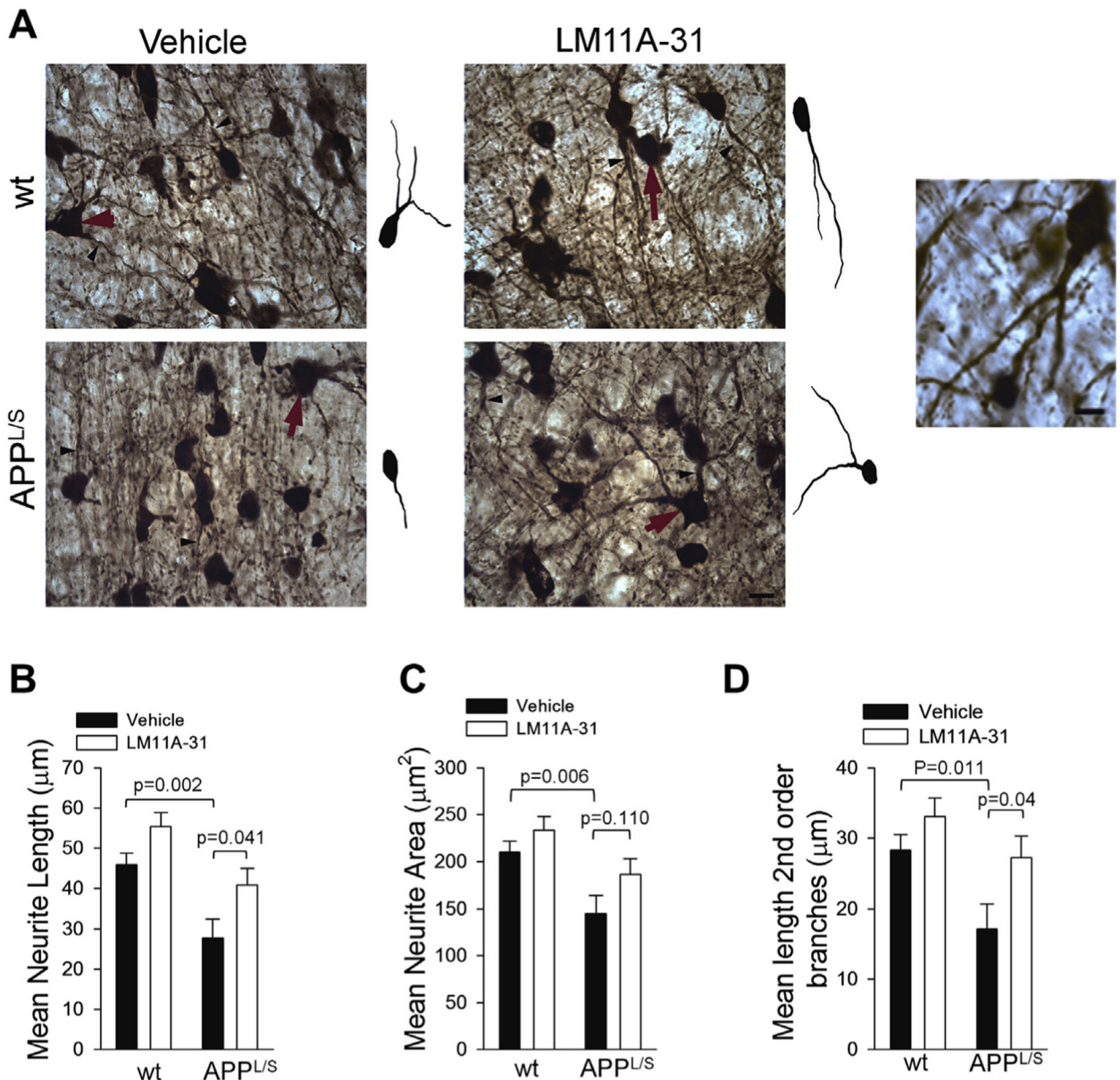
**Fig. 1.** LM11A-31 exhibits favorable brain bioavailability without toxicity. (A) LM11A-31 concentration was measured in brain and plasma of CD-1 mice after a single 50-mg/kg oral dose ( $n = 3$  mice per time-point). A peak brain concentration of 262 ng/g of brain tissue, or approximately 1.08  $\mu\text{mol/L}$ , well above the *in vitro* therapeutic dose of 100 nmol/L (Yang et al., 2008) occurred approximately 30 minutes post dose. The brain half-life of LM11A-31 was 3 to 4 hours. (B) C57BL/6 mice were treated with LM11A-31 for 2 weeks with 10 mg/kg/day ( $n = 3$  mice), 50 mg/kg/day ( $n = 5$  mice) or 100 mg/kg/day LM11A-31 ( $n = 4$  mice), then sacrificed 30 to 60 minutes after the last dose to assess peak brain concentration. Brain concentration in the 50 mg/kg/day group was 463.4 ng/g or approximately 1.9  $\mu\text{mol/L}$ . (C and D) After 9 days of treatment with LM11A-31 at 50 mg/kg/day ( $n = 9$  mice) or vehicle ( $n = 5$  mice), C57BL/6 mice underwent open field testing, which revealed no differences in ambulatory activity (C) or fine movements (D). (E) No weight changes were seen in the treatment groups depicted in C and D. Graphs represent the mean  $\pm$  SE.



**Fig. 2.** LM11A-31 prevents cognitive deficits. (A) LM11A-31 prevented novel object recognition (NOR) deficits in APP<sup>L/S</sup> mice. Bars depict mean ± SE, *p* values indicated (wt-vehicle, *n* = 14 mice; wt-LM11A-31, *n* = 11; APP<sup>L/S</sup>-vehicle, *n* = 7; APP<sup>L/S</sup>LM11A-31, *n* = 6). (B) Total exploration time in the NOR test did not vary significantly between treatment groups. (C) LM11A-31 prevented spatial working memory deficits (Y maze testing) in APP<sup>L/S</sup> mice (wt-vehicle, *n* = 8 mice; wt-LM11A-31, *n* = 8; APP<sup>L/S</sup>-vehicle, *n* = 8; APP<sup>L/S</sup>-LM11A-31, *n* = 10). Statistical significance was determined using ANOVA and post-hoc Student–Neuman–Keuls testing. (D) The total number of arm entries in the Y maze was similar between treatment groups.



**Fig. 3.** LM11A-31 does not affect number or size of basal forebrain cholinergic neurons. Unbiased stereological analysis was performed on choline acetyltransferase-immunostained basal forebrain sections from wt and APP<sup>L/S</sup> mice treated with vehicle or LM11A-31. Consistent with previous studies, APP<sup>L/S</sup> mice exhibited no change in cell number (A) or volume (B) relative to wt mice. We also detected no effect of LM11A-31 administration upon cell volume or number. Statistical significance was determined using ANOVA with post-hoc Student–Neuman–Keuls testing (wt-vehicle,  $n = 6$  mice; wt-LM11A-31,  $n = 6$ ; APP<sup>L/S</sup>-vehicle,  $n = 6$ ; APP<sup>L/S</sup>-LM11A-31,  $n = 6$ ).

**Fig. 4.**

LM11A-31 prevents degeneration of basal forebrain cholinergic neurites. (A) Representative photomicrographs of choline acetyltransferase-immunostained basal forebrain sections. Neurites (such as those indicated with arrowheads) were manually traced through 3 dimensions (x, y, z) while viewing tissue live, using Neurolucida software to derive quantitative data (only the x and y dimensions are shown). A representative neuron (indicated by a red arrow) in each of the 4 conditions is shown in *camera lucida* format derived from Neurolucida tracing. Scale bar = 20  $\mu\text{m}$ . Right,  $\times 40$  view of cholinergic neurites clearly emanating from a BFCN cell body, allowing accurate tracing from neurite origin. Scale bar = 10  $\mu\text{m}$ . Treatment of APP<sup>L/S</sup> mice with LM11A-31 was associated with increased length (B), and branching (D) of cholinergic neurites. There was a nonsignificant increase in surface area of neurites in APP<sup>L/S</sup> mice treated with LM11A-31

(C). Statistical significance was determined using ANOVA with post-hoc Student–Neuman–Keuls testing (wt-vehicle, n = 15 mice; wt-LM11A-31, n = 12; APP<sup>L/S</sup>-vehicle, n = 6; APP<sup>L/S</sup>-LM11A-31, n = 8).

Author Manuscript

Author Manuscript

Author Manuscript

Author Manuscript

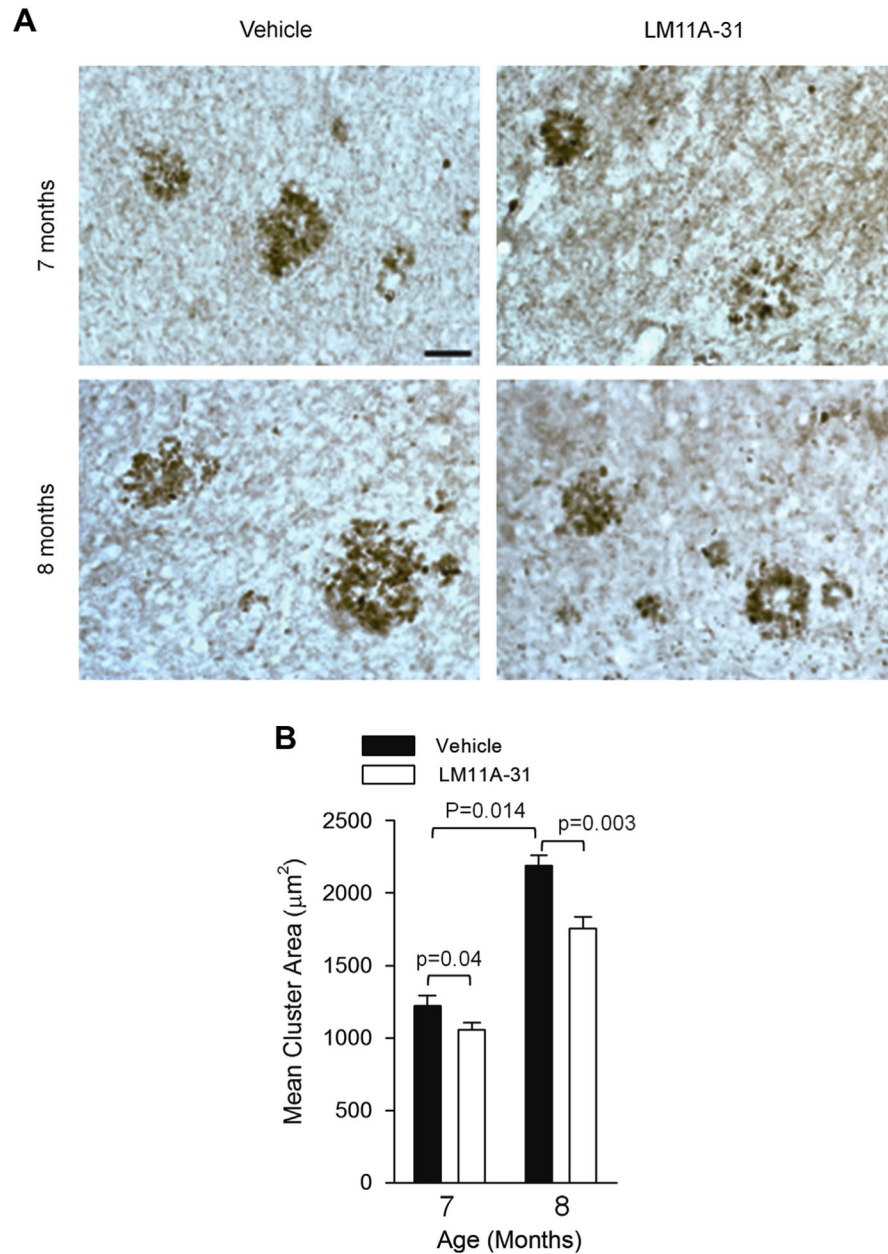


**Fig. 5.** LM11A-31 decreases cholinergic neuritic dystrophy in the cortex. (A) Representative photomicrographs of choline acetyltransferase-stained neurites in the cortex of 7-month (NOR cohort) or 8-month (Y maze cohort)  $\text{APP}^{\text{L/S}}$  mice treated with vehicle or LM11A-31 are shown. The area of dystrophic neurite clusters increases with age and is reduced by LM11A-31 treatment. (B) Quantitation shows an age-related increase in dystrophic neurite area as well as the protective effect of LM11A-31 in both age groups (7-month cohort:  $\text{APP}^{\text{L/S}}$  veh  $n = 8$ , mean age  $6.9 \pm 0.2$  months;  $\text{APP}^{\text{L/S}}$  LM11A-31  $n = 8$ , mean age  $6.9 \pm 0.1$  months. 8-month cohort:  $\text{APP}^{\text{L/S}}$  veh  $n = 5$ , mean age  $8 \pm 0.3$  months;  $\text{APP}^{\text{L/S}}$  LM11A-31  $n = 4$ , mean age  $8.1 \pm 0.5$  months).

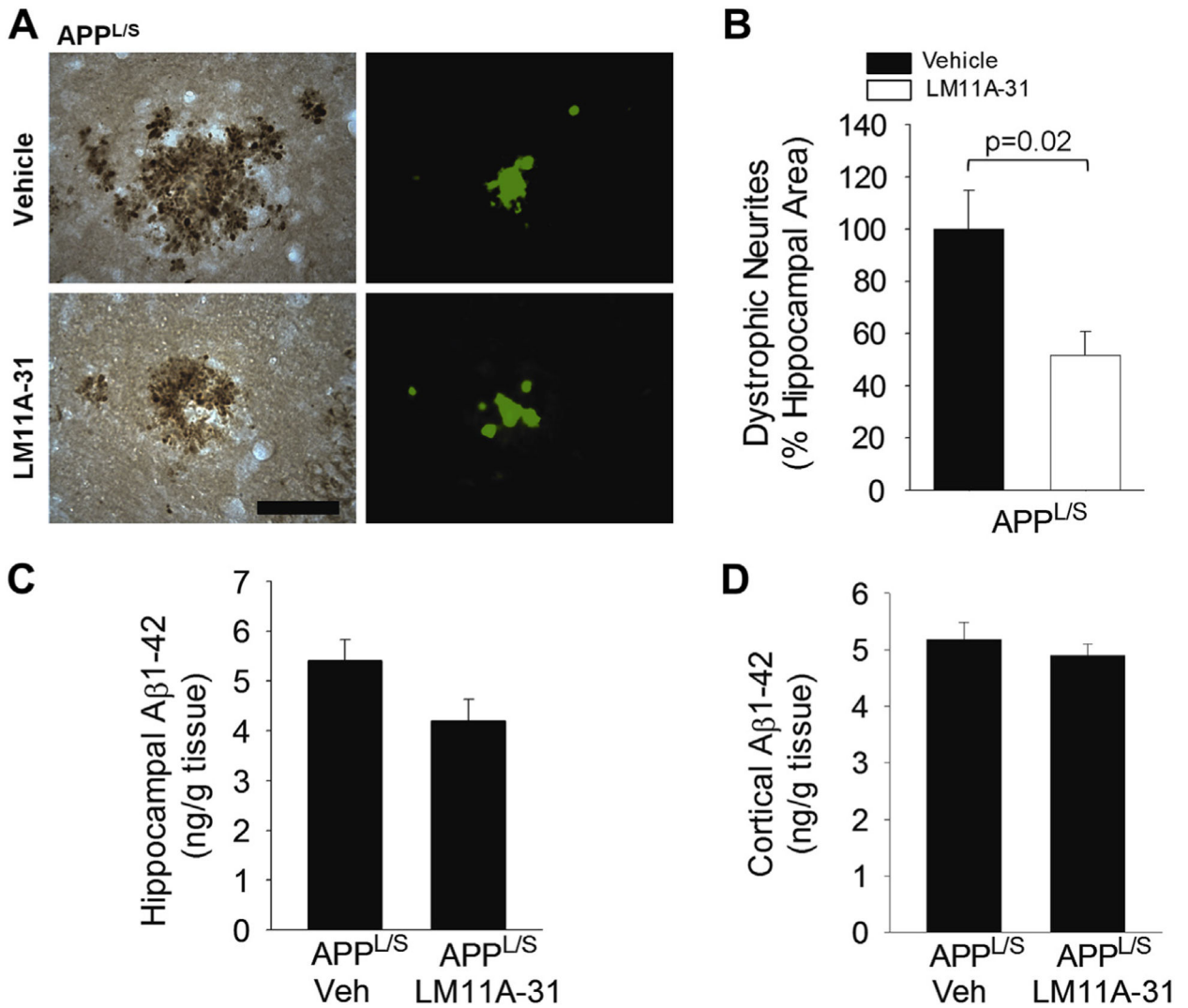


**Fig. 6.** LM11A-31 reduces neuritic dystrophy within the hippocampus without affecting amyloid beta levels. (A) Representative photomicrographs of APP immunolabeling for dystrophic neurites (left) and Thioflavin S staining for amyloid plaques (right) in hippocampi of  $APP^{L/S}$  mice given vehicle or LM11A-31 as indicated. Scale bar = 25  $\mu$ m. (B)  $APP^{L/S}$  mice treated with LM11A-31 ( $n = 6$ ) had decreased neuritic dystrophy compared to vehicle-treated mice ( $n = 5$ ;  $p$  value indicated, 2-tailed t-test). (C)  $APP^{L/S}$  mice treated with LM11A-31 ( $n = 6$ ) and vehicle ( $n = 6$ ) had similar amounts of A $\beta$ (1–42) in hippocampal tissue as determined by ELISA, non-significant by 2-tailed Student t-test. (D)  $APP^{L/S}$  mice treated with LM11A-31 ( $n = 8$ ) and vehicle ( $n = 8$ ) had similar amounts of A $\beta$ (1–42) in cortical tissue, nonsignificant by 2-tailed student t-test.



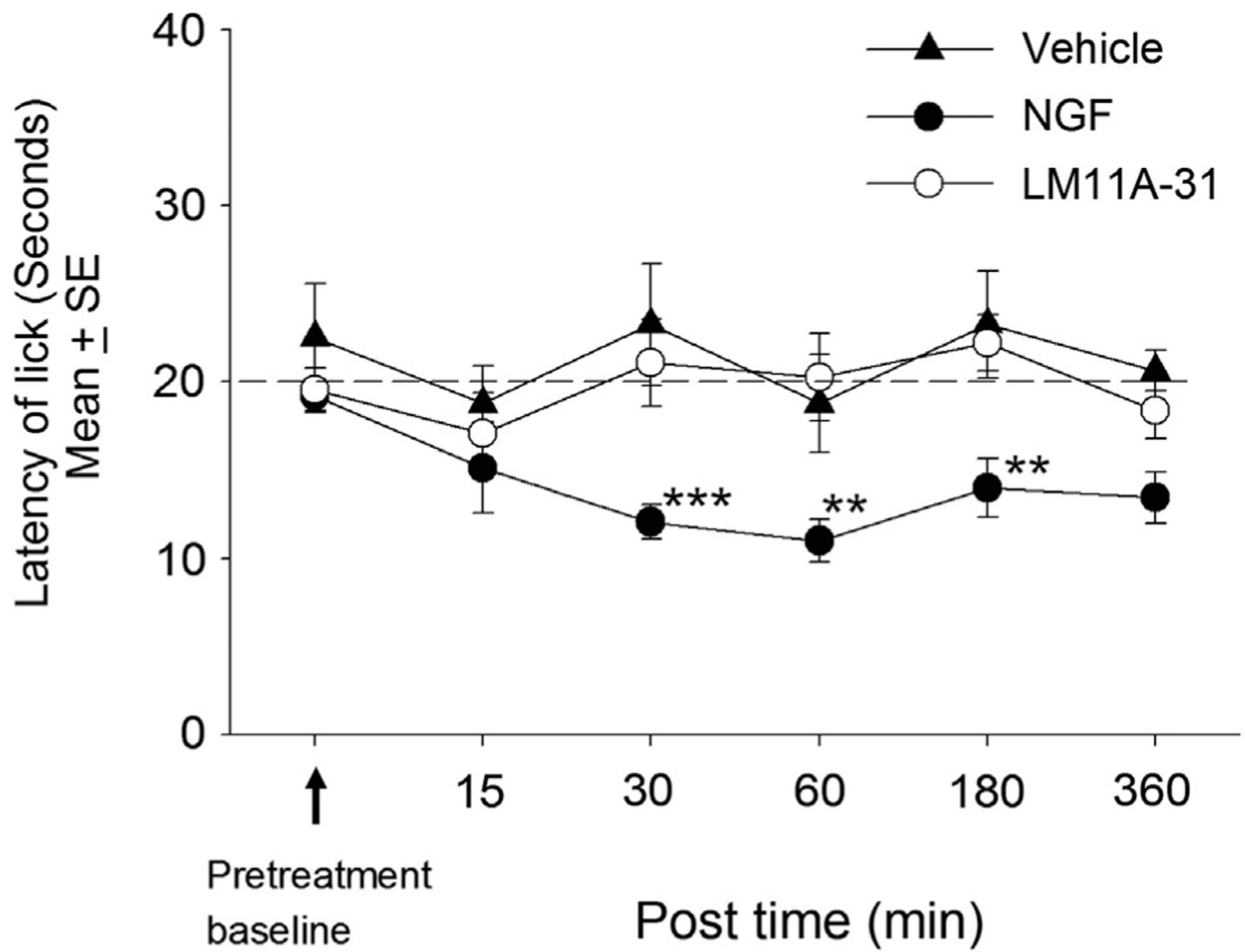


**Fig. 7.** NGF, but not LM11A-31, induces hyperalgesia. C57BL/6 mice were treated with IP injections of vehicle (n = 4), NGF 2.5 mg/kg (n = 8) or LM11A-31 20 mg/kg (n = 8), then placed on a hotplate at various time points after administration. Latency to paw licking behavior was significantly decreased at the time points indicated in animals treated with NGF while no effect was detected in animals treated with vehicle or LM11A-31. ANOVA with Student–Newman–Keuls multiple comparison method: \*\*  $p < 0.002$ ; \*\*\*  $p < 0.001$ .